# A system for measuring bubble voidage and frequency around tubes immersed in a fluidized bed of particles

Kevin J. Whitty and Michael Siddoway
*Department of Chemical Engineering, University of Utah, Salt Lake City, Utah 84112, USA*

(Received 9 July 2009; accepted 17 June 2010; published online 29 July 2010)

Gas-solid fluidized beds are common in chemical processing and energy production industries. These types of reactors frequently have banks of tubes immersed within the bed to provide heating or cooling, and it is important that the fluid dynamics within these bundles is efficient and uniform. This paper presents a simple, low-cost method for quantitatively analyzing the behavior of gas bubbles within banks of tubes in a fluidized bed cold flow model. Two probes, one containing an infrared emitter and one containing an infrared (IR) detector, are placed into adjacent glass tubes such that the emitter and detector face each other. As bubbles pass through the IR beam, the detector signal increases due to less solid material blocking the path between the emitter and detector. By calibrating the signal response to known voidage of the material, one can measure the bubble voidage at various locations within the tube bundle. The rate and size of bubbles passing through the beam can also be determined by high frequency data collection and subsequent analysis. This technique allows one to develop a map of bubble voidage within a fluidized bed, which can be useful for model validation and system optimization. © *2010 American Institute of Physics.*
[doi:10.1063/1.3462967]

## I. INTRODUCTION

Fluidized bed reactors, in which a bed of solid particles (e.g., sand) is "fluidized" by flowing a gas upwards though a reaction chamber, are common in the chemical processing industry and offer advantages for gas-solid reactions, including high interfacial area for reactions, thorough mixing throughout the reactor volume and excellent heat transfer. Gas flows through a fluidized bed either in the dense phase, between particles, or as low density bubbles, which can grow in a manner similar to bubbles rising through a liquid. The bubbles in a fluidized bed dictate the flow patterns in the reactor. Rising bubbles carry solids upwards in their wake and are ultimately responsible for mixing the solids throughout the bed.[1]

Due to the excellent heat transfer and uniform temperature profile that results from the thorough mixing and high surface area of the particles, fluidized beds are often used for reactions that require or generate significant amounts of heat. The overall temperature of the bed is maintained by adding or removing heat, typically through the use of heat exchange tubes located within the bed itself. For example, heat released during fluidized bed combustion of coal is used to generate steam in boiler tubes that are mounted inside the fluidized bed reactor. Removing heat in this manner keeps the bed from overheating and allows control of bed temperature.

It is important to understand how bubbles develop in fluidized beds and how they behave within bundles of horizontal tubes. It is known that bubbles traveling upwards in a fluidized bed grow as the solids head pressure decreases, and that bubbles can coalesce to form larger bubbles.[1–3] Upon contact with horizontal tubes, bubbles may travel between tubes if tube spacing is large enough, or they may split into two or more smaller bubbles. These "daughter bubbles" may coalesce to reform larger bubbles above the tube bank. The presence of horizontal tubes reduces the effective cross-sectional area of the bed, with the consequence that the superficial velocity increases and overall expansion of the bed results.[4]

Analyzing bubble flow patterns within fluidized beds is challenging, simply because the bed material obscures the view into the interior of the bed where the bubbles flow. Even with glass or acrylic cold-flow systems, one can only see a few millimeters into the dense phase of the bed. One approach that has been successfully employed is to create a thin, nearly two-dimensional fluidized bed between two plates of transparent material and to analyze images or videos of the bed during operation.[5–7] This technique and associated data analysis is relatively straightforward, but restricting one dimension does not allow bubbles to grow in a natural manner and applicability of results to three-dimensional systems is questionable. A common method of studying hydrodynamic behavior in three-dimensional beds is to measure pressure fluctuations at specific locations and to infer bubble size and frequency based on the magnitude, duration, and frequency of the fluctuations.[8–10] Resolution is limited by the speed of the pressure transducer and pressure dampening that occurs between the pressure tap and transducer. Pressure measurements are also not very feasible for measuring bubble behavior in banks of horizontal tubes. To better understand the interaction between bubbles and horizontal tubes, Yates *et al.*[11,12] performed x-ray measurements to track the behavior of a single bubble in a three-dimensional bed with horizontal tubes. Their work provided useful insight into splitting and recombination of one bubble

 

as it travels through a bank of horizontal tubes, but does not indicate how a bed full of bubbles of different sizes behaves. Still another technique used for analysis of hydrodynamics in fluidized bed systems is capacitance-based imaging and tomography, which uses transmission of oscillating electrical signals among an array of electrodes within the bed to deduce the voidage profile at high temporal resolution.[13–17] Capacitance imaging allows mapping and evaluation of hydrodynamics of an entire bed at relatively low cost, but resolution is limited and flow of bubbles through a bank of horizontal tubes cannot be mapped.

Optical methods have been used to quantify properties of individual bubbles in fluidized beds. Glicksman *et al.*[18] and Farrell and Glicksman[19] used an infrared transmitter-detector pair to identify the presence of bubbles in a cold flow fluidized bed. By installing two such pairs above one another and measuring the time between observation of bubbles, bubble rise velocity could be calculated. Bubble fraction could also be estimated by calibrating detector sensitivity against a theoretical model of bubble fraction at the measurement location. This technique proved useful for characterization of specific locations within a bed. Reh and Li[20] used a similar optical probe to identify how voidage at specific locations in a bed varies with operating conditions. More recently, Mainland and Welty[21] used a probe incorporating fused quartz rods to direct a beam of infrared light across a gap to study bubble behavior in fluidized beds operating as hot as 1200 K. These studies all advanced the understanding of bubble behavior in open areas of the bed where probes can be easily positioned. However, the intrusive design of these probes makes evaluation in the tube bank region of a bed challenging.

The technique described in this paper overcomes this limitation and expands optical analysis of fluidized bed behavior to allow three-dimensional mapping of voidage, bubble size, and bubble frequency throughout tube bank regions of fluidized beds. The equipment is very simple and low cost, and evaluation and interpretation of data is straightforward.

## II. APPARATUS

The experimental system for measuring bubble voidage and frequency comprises three components: a fluidized bed, a pair of probes for detecting bubbles within the bed, and the data acquisition system. These are described below.

### A. Fluidized bed

The fluidized bed that was analyzed is a scaled down cold-flow model of an indirectly heated development-scale fluidized bed gasifier located at the University of Utah. Procedures for scaling down fluidized bed systems are well established and involve matching a set of four dimensionless parameters describing: (1) the ratio of inertial to viscous forces, (2) the ratio of inertial to gravitational forces, (3) the ratio of solid and gas densities and (4) the ratio of bed depth and diameter.[1] The fluidized bed is modular in design and constructed from several pieces of acrylic tube [178 mm outer diameter (OD) × 165 mm inner diameter (ID)] that can be stacked and rotated to allow different overall geometries. To represent the heater bundles in the gasifier, four identical tube bundle sections were manufactured. Each section contained 20 borosilicate glass tubes (11 mm OD, 7 mm ID) extending across the diameter of the bed in a five tube wide by four tube high, vertically staggered, triangular pitch configuration (Fig. 1). Center-to-center distance between adjacent tubes is 21 mm, resulting in spaces between tubes that were slightly less than one tube in diameter. Each tube bundle section is 95 mm high and the four sections are positioned perpendicular to one another as in the fluidized bed gasifier that was being modeled. A 356 mm long section of acrylic tube representing the bottom region of the gasifier is installed below the bottom tube bundle.

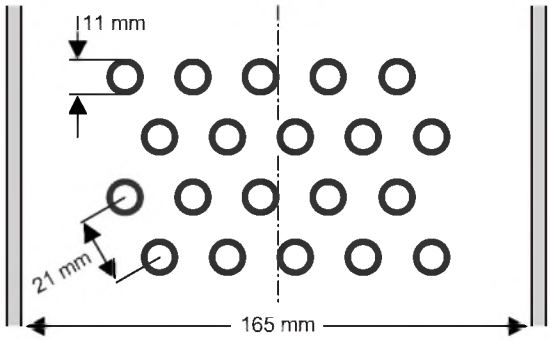


FIG. 1. Configuration of the glass tubes in the cold-flow fluidized bed described in this study.

Air is introduced into the bottom of the fluidized bed through a distributor comprising a plenum below two 3 mm thick metal plates each having 42 14 mm holes drilled at even spacing. Two layers of high-density fabric are sandwiched between the two plates to create sufficient pressure drop to ensure even air distribution.

The particles that formed the fluidized bed were beads of soda-lime silica glass (Potters Industries). The beads were very spherical and nearly transparent, which is important for the bubble detector. Several size ranges, 70–110, 180–250, and 500–750 $\mu$m, have been tested.

### B. Bubble detector

The bubble detector comprises a pair of probes that measure the amount of infrared light transmitted between adjacent tubes. One probe contains a side-looking Fairchild Semiconductor QEE123 AlGaAs high output infrared light-emitting diode (LED). The transmitter wavelength spans roughly 775–985 nm, centered and most strong at 880 nm. The emission angle of the LED is approximately 50°. The transmitter is powered with an adjustable dc power source capable of delivering between 0 and 5 V.

The other probe contains a side-looking Fairchild Semiconductor QSE114 phototransistor capable of delivering between 0 and 5 V depending on the amount of light received. The phototransistor has a view angle of 50° and is coated with a daylight filter to avoid interference from visible light. This makes it possible to conduct experiments with the laboratory lights on without concern of interference. It was con-

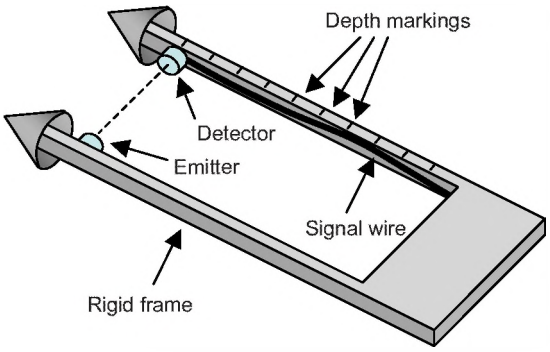


FIG. 2. (Color online) Frame system used to secure the IR emitter and detector. The cones on the end have the same diameter as the insides of the glass tubes, thereby ensuring that the arms of the frames are centered and in the same position between measurements.

firmed that turning laboratory lights on does not affect the output of the phototransistor.

The two probes are mounted on a frame which ensures that their separation distance and orientation remain fixed (Fig. 2). The whole probe assembly can be inserted such that the transmitter and detector are in adjacent tubes, and can be inserted to the desired depth. Plastic cones at the tips of the probes ensure that the transmitter and detector remain centered within the tubes.

### C. Data acquisition system

The 0–5 V signal output from the phototransistor sensor is coupled to a LABJACK U12 data acquisition system capable of sampling at a frequency of 1200 Hz. Voltage output data are acquired using the LABJACK software which bundled with the U12 system and is logged to a data file. After the experiment is over, this file is imported into MICROSOFT EXCEL and calculations are performed to determine bubble frequency, bubble voidage, and relative bubble size.

## III. EXPERIMENTAL PROCEDURE

Measurement of bubble voidage and frequency involves measurement calibration, data acquisition, and postexperimental data analysis.

### A. Calibration

Prior to each measurement campaign, the probe system must be calibrated to ensure that voidage measurements are correct and that the amount light transmitted to the sensor covers its range of sensitivity. A special calibration apparatus comprises two of the glass tubes vertically spaced the same distance apart as in the fluidized bed system (21 mm center-to-center). These tubes are immersed in a bed of solids at a slight angle so that one end of the tubes is completely covered while the other end is uncovered, and that the amount of solids between the tubes varies linearly (Fig. 3). We have found that it helps to vibrate the calibration bed slightly to level the surface of the particles. This also helps ensure tight packing of the particles.

The first step of the calibration involves inserting the probes deep enough into the tubes that both are covered with solids. The power of the IR transmitter is adjusted so that a

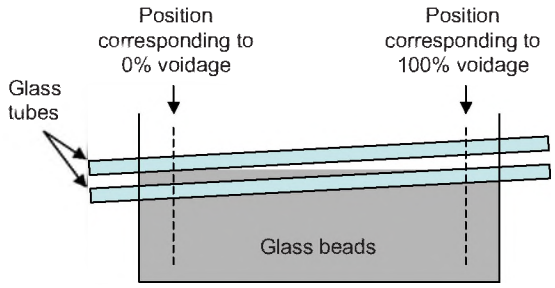


FIG. 3. (Color online) System used for calibrating the response of the detector as a function of bubble voidage in the bed. At 100% voidage, there are no particles between the two tubes. At 0% voidage, the space between the tubes is fully packed with particles.

weak signal is received by the detector. This ensures that one extreme—that of completely packed bed with no voidage other than the minimum interparticle voidage—falls within the range of measurement. The second calibration step involves measuring signal received at different locations within the tubes and recording sensor signal strength versus voidage between the tubes, defined as the fraction of the intertube distance above the level of the particle bed. Approximately 20 data points are taken. The resulting curve is not linear, but instead is S-shaped as seen in Fig. 4. Between 0% and 35% voidage, when the bed is mostly packed, the received signal is mildly sensitive to changes in voidage and typically varies by about 0.05 V over this range. The inset magnification of that portion of the calibration curve shows this part of the curve in detail. Our experience is that the slope of this portion of the curve is steeper for smaller particles. At intermediate voidage, between roughly 35% and 85%, the signal varies strongly as a function of voidage. At very high voidage, the signal is near the maximum and does not vary significantly with changes in voidage. Generally, measured voidage during experiments is in the 15%–40% range. It is possible to improve the sensitivity of the detector by increasing the IR transmitter power such that the detector gives a maximum signal (for our system, 5 V) at 50%–60% voidage if higher voidage is unlikely or uninteresting. In order to maximize accuracy of the measurements, the

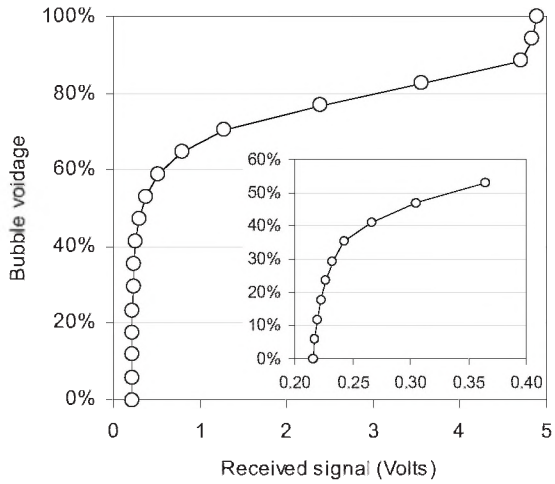


FIG. 4. Calibration curve of bubble voidage vs voltage received from the detector. The inset shows a magnification of the left part of the curve.

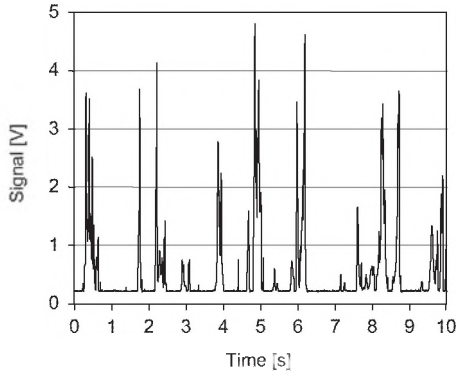


FIG. 5. Signal vs time for a typical 10 s period at a location near the center of the horizontal tube array. Spikes correspond to bubbles passing through the path of the IR beam.

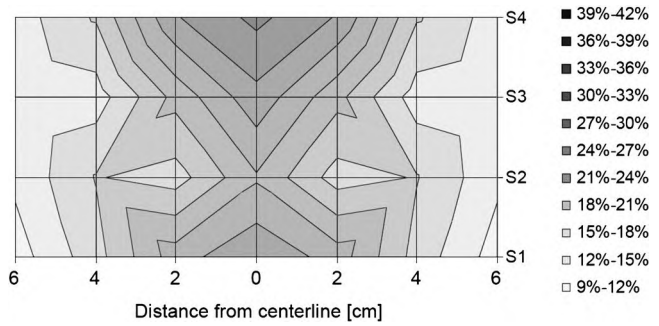


FIG. 6. Surface plot showing measured average bubble voidage across a horizontal plane within the tube bundle region of the fluidized bed. The indications S1–S4 indicate the four spaces between the five tubes at this level, which are oriented left-to-right.

response-versus-voidage data are treated as two curves, one from 0% to the inflection point at roughly 85% voidage and one at higher voidage, and polynomial equations are fit to each portion. During data interpretation, an IF( ) statement determines which calibration curve to use.

This calibration technique is representative of single bubbles flowing between adjacent tubes and may misrepresent conditions in which two or more bubbles cross the optical path simultaneously. However, for most practical fluidized bed systems, horizontal tubes (e.g., heat exchange tubes) are positioned high enough above the distributor that bubbles have grown to diameters larger than the spacing between tubes.[1,2] Consequently, the likelihood of two or more bubbles simultaneously passing between adjacent tubes is small.

### B. Data acquisition

Once calibration for a specific set of particles is complete and the transmitter power has been appropriately adjusted, experimental data acquisition can begin. One measurement of bubble voidage and bubble frequency involves operating the fluidized bed under the desired conditions (particle size, fluidizing gas flow rate, bed height) for 1 or 2 min to ensure steady conditions. The transmitter and phototransistor probes are positioned in the two tubes of interest at the desired location along the length of the tubes, taking care to ensure that the probes remain aligned such that the transmitter and sensor face each other. Data are then logged using the LABJACK software for 30–40 s at a frequency of 600 Hz. The probes can then be repositioned within the tubes or moved to a new set of tubes and a new data set can be logged at this position.

### C. Data analysis

The raw data are an array of the voltage signal received from the phototransistor versus time. For 35 s of sampling at 600 Hz, this results in about 20 000 data points. A sample of the raw signal generated by the phototransistor is shown in Fig. 5. The bubble voidage corresponding to the voltage is calculated for each data point using the equations developed in the calibration procedure. The average bubble voidage is calculated by integrating the area under the voidage-versus-time curve and dividing by the total sampling time.

A crude measurement of bubble frequency can be performed by counting the number of times the bubble voidage exceeds a designated minimum void fraction, typically 5%–15%, and then falls below the threshold again. Adjusting the cutoff frequency allows one set the "size" of bubble that will be included in the count. In theory, one should be able to perform crude bubble size distribution by varying the cutoff threshold over a given period of time. For example, for a 10 s sample one might count five "large" bubbles, determined by a high cutoff threshold. If this minimum bubble size is decreased and 12 bubbles are counted, then there would be the five large bubbles plus an additional seven medium bubbles. An additional threshold decrease that resulted in 20 total bubbles would indicate eight small bubbles. In practice, we have found that this approach of determining bubble size distribution does not work well because the bubbles are not well segregated and two or small bubbles may exist within the probe pair's line of sight.

The focus of the voidage studies is to identify how bubbles flowing upwards in fluidized beds move through banks of horizontal tubes. To characterize the whole bed, it is necessary to make voidage measurements at many locations. In our studies, measurements are typically taken in each tube at four locations: near the wall, in the center, and at two locations in between. Symmetry is assumed around the center point, so in effect seven data points are acquired. The fluidized bed being studied has five tubes at each of 16 levels. The five tubes offer four spaces through which to take measurements, so 16 measurements are taken at each level. The twelve points not on the centerline are symmetrically duplicated, resulting in 28 data points.

To interpret all data at a given level, we created both two-dimensional (2D) and three-dimensional (3D) surface plots, which joined the $x$-$y$ points together to make a virtual surface on which the color or intensity varies with voidage (2D plots) or the height of the surface is proportional to voidage.

## IV. EXPERIMENTAL RESULTS

A typical voidage plot is shown in Fig. 6. This plot was created using MICROSOFT EXCEL's charting feature and

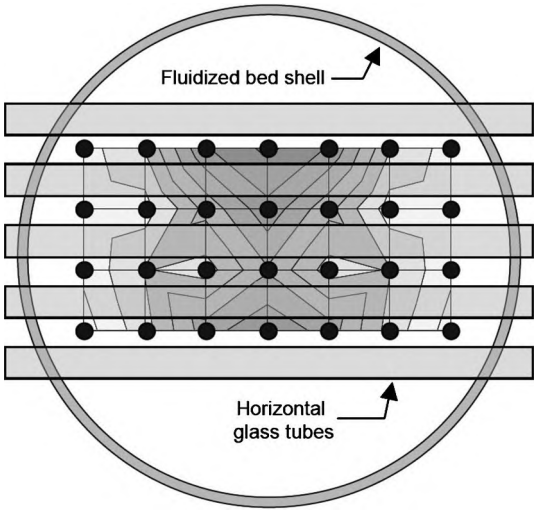


FIG. 7. Horizontal cross-section of the fluidized bed showing the voidage profile from Fig. 6. The black circles indicate the locations between the horizontal tubes where measurements were taken. The highest voidage is observed closest to the open spaces on the sides of the tube bundle where resistance to bubble flow is lowest.

choosing "surface" as the type of plot. The 28 data points from which the plot is constructed represent average bubble voidages calculated as described above. The lines S1–S4 represent the four spaces between the five horizontal tubes at this level (i.e., the tubes run from left to right). The distance from the centerline of the horizontal tubes is indicated on the bottom axis. The magnitude of bubble voidage is represented by the intensity of shading, with darker regions corresponding to less voidage and lighter regions corresponding to higher voidage. Higher voidage is an indication that more bubbles passed through that region.

For the case shown in Fig. 6, bubble voidage varied between 14% and 37%. The highest voidage was nearest the outside tubes, along the midpoint of the tubes. This makes sense once the relationship of the measurement locations to the overall bed is understood. Figure 7 depicts a cross-section of the fluidized bed at the level where the data are taken. The five horizontal tubes are shown as well as the bubble voidage profile between the tubes. Bubbles rising through a fluidized bed tend to migrate to areas with the lowest pressure drop and fewest restrictions. Clearly, the open areas on the sides of the tube bundles (top and bottom in the figure) present less resistance than the tube bundles. It is not possible to measure voidage in the area on the sides of the bundles using the technique presented here, but increased voidage near this region is apparent in Fig. 7.

The above results represent a single horizontal plane only. Compiling data for all planes offers a more complete picture of how bubble voidage varies throughout the bed, and offers insight into the flow patterns of the bubbles. This tool can be used to identify stagnant regions within horizontal tube bundles of fluidized beds, and can be used to help optimize bundle configuration in a cold flow model before a full-scale system is constructed.

## V. SUMMARY

The technique described in this paper offers a simple, low-cost method for quantitatively measuring bubble intensity and behavior within a bank of horizontal tubes in a fluidized bed. By making multiple measurements in three dimensions within a bundle of tubes, maps of bubble density and bubble frequency can be generated. The technique can be used to evaluate and optimize performance of heat exchangers within fluidized beds, and provides a quantitative method of acquiring validation data for computational models of fluidized bed systems.

## ACKNOWLEDGMENTS

This work was funded by the U.S. Department of Energy through cooperative agreement DE-FC26-02NT41490. The authors thank Thermochem Recovery International (TRI, Inc.) for valuable discussions during performance of this project.

[1] D. Kunii and O. Levenspiel, *Fluidization Engineering*, 2nd ed. (Butterworth-Heinemann, Newton, 1991).
[2] F. A. Zenz and D. F. Othmer, *Fluidization and Fluid-Particle Systems* (Reinhold Publishing, New York, 1960).
[3] J. A. Valenzuela and L. R. Glicksman, Powder Technol. **44**, 103 (1985).
[4] L. R. Glicksman and T. Yule, Chem. Eng. Sci. **46**, 1561 (1991).
[5] L. G. Jodra, J. M. Aragon, and J. Corella, Int. Chem. Eng. **19**, 654 (1979).
[6] P. K. Agarwal, A. S. Hull, and K. S. Lim, in *Noninvasive Monitoring of Multiphase Flows*, edited by J. Chaouki, F. Larachi, and M. P. Dudukovic (Elsevier, New York, 1996), p. 407.
[7] A. S. Hull, Z. Chen, J. W. Fritz, and P. K. Agarwal, Powder Technol. **103**, 230 (1999).
[8] O. Sitnai, S. C. Dent, and A. B. Whitehead, Chem. Eng. Sci. **37**, 1429 (1982).
[9] P. A. Olowson, Chem. Eng. Sci. **49**, 2437 (1994).
[10] J. Wiman and A. E. Almstedt, Chem. Eng. Sci. **52**, 2677 (1997).
[11] J. G. Yates and R. S. Ruiz-Martinez, Chem. Eng. Commun. **62**, 67 (1987).
[12] J. G. Yates, R. S. Ruiz-Martinez, and D. J. Cheesman, Chem. Eng. Sci. **45**, 1105 (1990).
[13] J. S. Halow and P. Nicoletti, Powder Technol. **69**, 255 (1992).
[14] J. S. Halow, G. E. Fasching, P. Nicoletti, and J. L. Spenik, Chem. Eng. Sci. **48**, 643 (1993).
[15] V. Wiesendorf and J. Werther, Powder Technol. **110**, 143 (2000).
[16] W. Q. Yang and L. Peng, Meas. Sci. Technol. **14**, R1 (2003).
[17] S. E. Olsson, J. Wiman, and A. E. Almstedt, Chem. Eng. Sci. **50**, 581 (1995).
[18] L. R. Glicksman, W. K. Lord, and M. Sakagami, Chem. Eng. Sci. **42**, 479 (1987).
[19] P. A. Farrell and L. R. Glicksman, Proceedings of the 14th International ASME Conference on Fluidized Bed Combustion, Vancouver, Canada, 1997, Vol. 2, p. 733.
[20] L. Reh and J. Li, in *Circulating Fluidized Bed Technology III*, edited by P. Basu, M. Horio, and M. Hasatani (Pergamon, Oxford, 1991), p. 163.
[21] M. Mainland and J. R. Welty, AIChE J. **41**, 223 (1995).